Guided complex waves
Part 1. Fields at an interface

T. Tamir, Ph.D., Associate Member, and Prof. A. A. Oliner, Ph.D.

Summary

The variety of waves which can be supported by a plane homogeneous interface includes surface waves of the forward and backward type, and several kinds of complex wave, the latter being characterized by wave numbers which are complex even though the media involved are not necessarily lossy. The present study views all these waves as contributions due to poles in several alternative integral representations of a source-excited field, and places particular stress on the steepest-descent representation. The pole locations, field distributions and power-transport properties are explored in detail for all the wave types. Distinctions are made between proper (spectral, modal) and improper waves, and between lossy and lossless structures; complex waves along lossless structures are shown to appear always in degenerate pairs consisting of a forward and a backward wave, with interesting power-flow characteristics. The different wave types are grouped into the general category of guided complex waves which propagate without attenuation as inhomogeneous slow plane waves at some angle to the interface. Power-transport considerations via the steepest-descent representation show that these waves either carry power to compensate for losses in the system or account for a transfer of energy into the radiation field.

List of symbols

c = Velocity of light in free space
$f(\kappa)$ = Complex amplitude function for the κ-mode
$G(x, z)$ = Total solution for the field in Cartesian co-ordinates
$G_p(x, z)$ = Pole contribution to $G(x, z)$
$G(r, \theta)$ = Total solution for the field in polar co-ordinates
$G_p(r, \theta)$ = Pole contribution to $G(r, \theta)$
$G_s(r, \theta)$ = Space-wave contribution to $G(r, \theta)$
$G_0(\phi_p)$ = Field contribution at the origin due to a pole at $\phi = \phi_p$
$k = \omega(\mu_0\epsilon_0)^{1/2}$ = Wave number of plane wave in free space.
P_x, P_z = Components of power flow
r = Radial field co-ordinate
v_g = Group velocity
v_p = Phase velocity
x, y, z = Cartesian field co-ordinates
$Z_i(\kappa)$ = Impedance at the interface
$Z_0(\kappa)$ = Characteristic impedance of transmission line representing free space
α_r = Radial attenuation factor
β_r = Radial phase factor
ϵ_0 = Absolute permittivity of free space
$\zeta = \zeta_r + j\zeta_i$ = Wave number in the z-direction
$\zeta_p = \zeta_{pr} + j\zeta_{pi}$ = Location of a pole in the complex ζ-plane
η = Imaginary component of ϕ
η_p = Imaginary component of ϕ_p
θ = Angular field co-ordinate
θ_c = Angle of definition for pole contributions
$\kappa = \kappa_r + j\kappa_i$ = Wave number in the x-direction
$\kappa_p = \kappa_{pr} + j\kappa_{pi}$ = Location of a pole in the complex κ-plane
μ_0 = Absolute permeability of free space
ξ = Real component of ϕ
ξ_p = Real component of ϕ_p
ϕ = The steepest-descent complex variable
ϕ_p = Location of a pole in the complex ϕ-plane
ω = Angular frequency

Paper 4036E, first received 19th March and in final form 7th August 1962

Dr. Tamir and Prof. Oliner are at the Microwave Research Institute, Polytechnic Institute of Brooklyn, New York

1 Introduction

The discrete modes of propagation along guiding systems were studied extensively for both closed and open (radiating) structures. In lossless conventional waveguides the modes proved to represent waves which either propagate without attenuation or decay exponentially without any phase change. Along open lossless structures, on the other hand, a continuous spectrum of modes was found, in addition to a discrete set, if any; the latter accounted for the various types of 'surface waves',[1-5] while the continuous spectrum had a direct bearing on radiation. Both open and closed configurations were characterized by propagation coefficients which were either purely real or purely imaginary, and this was demonstrated[6] to apply to all structures which contain lossless, isotropic and dispersionless media only.

When the condition of zero loss is removed, modes appear whose wave number is complex rather than real or imaginary, and the wave then propagates with attenuation due to power being absorbed into the lossy medium. In closed waveguides, these losses are generally of an unwelcome and annoying feature, but in open structures they sometimes proved to be useful, in that they made possible the propagation of some types of surface wave.[3,4,7] Since Sommerfeld's study[1] of waves along a lossy wire, and until recently, these waves were the only modes of propagation with which a complex wave number was associated, and some controversy on the correct interpretation of one of them, the Zenneck wave,[2] has been in progress for some time; however, in so far as the propagation and power transport are concerned, these waves seem to be well understood,[3] and they can easily be explained in terms of the losses in the systems considered.

Another type of complex wave* investigated recently is the non-modal 'leaky' wave[8-10] which may appear on open structures even when no losses are present; this wave, however, is improper, since it violates the radiation condition at infinity and can therefore exist in restricted regions only.

More recent work has shown that proper, i.e. modal, spectral, complex modes are possible in structures containing anisotropic[11-13] or dispersive[13,14] media, with or without losses; these waves are independent solutions of the homogeneous equation, subject to all the boundary conditions,

* The term 'complex wave' will henceforth be applied to all waves for which the propagation coefficient is complex, rather than real or imaginary

including the radiation condition. It is shown here, via a steepest-descent representation, that some of these waves are significant in radiation problems in a manner that was hitherto associated only with the improper complex waves. It is thus demonstrated that the energy leakage from open structures is related to the existence of certain guided complex waves which are not necessarily improper solutions of the wave equation. The term 'leaky wave' should therefore be extended to include all complex waves which exhibit the feature of energy transfer into the radiation field, to distinguish them from those complex waves which take account of power being carried to compensate for losses in the system. From this standpoint, the distinction between proper and improper waves is seen to be purely formal, since leaky waves may actually belong to either type.

In the present paper, particular attention has been paid to open structures, because the complex waves supported by them are more interesting and rewarding. The present investigation therefore deals with a semi-infinite free-space region bounded by a plane interface with boundary conditions of a rather general type, which are described in Section 2. A similar problem was considered by Brown,[15] who discussed, however, a more restricted situation involving only a continuous spectrum and surface waves; non-modal leaky waves were not discussed, and complex modes did not exist in the configuration investigated by him.

The classification of wave types employed here differs from that of Karbowiak.[16, 17] The 'quasi-modes' of Karbowiak denote all wave types other than the well-defined modes of conventional ideal waveguides and lossless surface waveguides. He is concerned primarily with imperfect waveguides, where his point of view offers a conceptual advantage; his quasi-modes may, in such a context, be either proper or improper solutions of the wave equation, or may not even satisfy the wave equation exactly. In contrast, we restrict our discussion to various canonical wave types. Most of our complex waves would constitute examples of quasi-modes, but we are careful to distinguish between proper and improper solutions, and cases for which loss is or is not present. In fact, we stress that important differences are present in the properties of the various wave types because of these distinctions.

Two alternative integral representations for the total field excited by a line source are examined in the present study:

(*a*) A longitudinal spectral representation in terms of modes along the interface, with propagation normal to this interface.

(*b*) A transverse spectral representation of modes, in the perpendicular cross-section, with propagation along the interface.

The integrand of these representations may contain poles, which are assumed to be simple, and these account for the various types of wave examined herein. Although the discussion of these alternative representations does not present basically new aspects, it is included here to furnish a suitable foundation for defining terms and concepts, as well as for presenting the various wave types and some of their interrelations which were not known or appreciated hitherto.

The significance of the radiation condition at infinity is emphasized both in the choice of a particularly suitable branch cut for the integral representations and in classifying the pole contributions as proper (spectral) or improper (non-spectral). Although only the former may contribute to the spectral representations, both types may contribute to the field in a steepest-descent representation, which is described next. It is primarily this last representation that is employed in the present paper, since it provides an asymptotic result which is convenient for many physical interpretations and, in particular, permits certain power-transport considerations which explain features of the radiation field.

In the light of concepts derived from the various integral representations, the properties of the pole contributions are discussed in Section 3. It is shown that the complex waves due to any pole, whether proper or improper, in lossy or in lossless structures, are always special cases of a general complex wave whose properties depend mainly on the location of the particular pole in the complex plane. All these various waves are examined separately and their fields are described. Pole contributions always appear as slow plane inhomogeneous waves propagating at an angle to the boundary interface; this angle is always non-zero if losses are present. For lossless media, however, the angle may become zero, and then the complex wave is actually a true surface wave bound to, and propagating unattenuated along, the interface; although the term 'surface wave' has been used by others to include evanescent waves along lossy structures,[3–5] it is used here to denote only non-attenuating waves bound to, and propagating along, the interface between lossless media.

It is shown that a characteristic feature of lossless media is that complex waves, if they are present, appear in pairs; with proper complex waves, the waves of a pair are degenerate modes since they are not orthogonal to each other.* One of these is identified as a forward wave and the other as a backward wave; these waves are so excited that complete real-power cancellation occurs. In a similar manner, true surface waves may also be of the forward or backward type, but they do not necessarily occur in pairs and, if they do, they are not degenerate but are orthogonal to each other. Although the forward surface waves are familiar, the backward wave is novel in non-periodic systems and was shown to exist only recently.[14, 18–25] The presence of such backward modes is shown to require a careful consideration of the path of integration in the integral representations. The effect of a unidirectional source, rather than the more common bidirectional one, is also treated, and the asymmetry thus introduced in the field is shown to emphasize the backward character of some of the spectral complex waves.

Finally, the power flow associated with complex waves is treated in Section 4; it is shown that in a steepest-descent representation the energy of a complex wave is either carried in to the radiation field, where it may account for peaks in the radiation pattern, or is given up to compensate for losses in the system. These considerations enable one to predict certain features of the radiation pattern when the location of the pole in the complex plane is known. This aspect is treated more extensively in a companion paper.[26]

2 Alternative field representations

The class of geometrical configurations considered here is illustrated in Fig. 1; it consists of a semi-infinite free-space region bounded by a plane surface, referred to hereafter as the interface. This interface may be either a true boundary, e.g. a reactive surface, an ideal conductor, a lossy sheet, etc., or it may represent a transition boundary between the free-space region and other specified media; e.g. the interface may be the upper surface of a slab or of a combination of stratified media. If the boundary condition at this interface is assumed to be independent of the y and z co-ordinates, it may then be expressed as an impedance function $Z_i(\kappa)$ which is specified at the interface for every single mode in the transverse x-direction and is invariant with respect to y and z; κ then denotes a variable which characterizes the mode in question. For simplicity, it will be assumed that the sources present are homogeneous in

* No orthogonality condition exists for improper waves

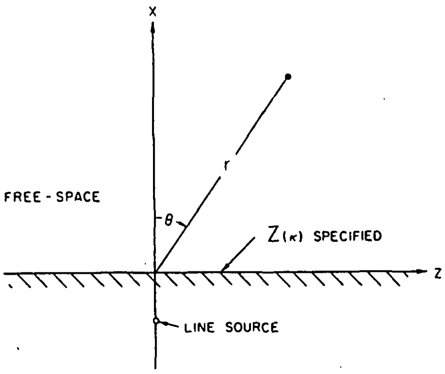

Fig. 1
Geometry of the plane interface

the y-direction, so that the fields excited are two-dimensional only ($\partial/\partial y = 0$)

2.1 The longitudinal spectral representation

The solution of a Green's function problem is investigated here by customary procedures; in agreement with the prescribed y-invariance, the source is taken as a line current of either the electric or magnetic type, located at $z = 0$ and parallel to the y-axis. The field at and above the interface ($x \geqslant 0$) is then given as

$$G(x, z) = \frac{1}{2\pi}\int_{-\infty}^{\infty} f(\kappa)\varepsilon^{j\kappa x}\varepsilon^{j\zeta z}d\zeta \quad . \quad . \quad . \quad (1)$$

with a time dependence $\varepsilon^{-j\omega t}$ understood. Then $G(x, z)$ is proportional to the y-component of the magnetic (E-mode) or electric (H-mode) field excited, respectively, by electric or magnetic line currents. It is clear that $G(x, z)$ expresses the field as a Fourier transform with respect to ζ, the integration being carried out along the real axis in the complex ζ-plane. The variables κ and ζ denote the wave numbers in the x- and z-directions, respectively, and they are related by

$$\zeta = \pm\sqrt{(k^2 - \kappa^2)} \quad . \quad . \quad . \quad . \quad . \quad (2)$$

where $k = \omega(\mu_0\epsilon_0)^{1/2}$ is the propagation wave number of plane waves in free space. The term $f(\kappa)$ acts as a weight or amplitude function which depends both on the impedance function $Z_i(\kappa)$ specified at the interface and on the location of the source.

It is recognized that the field as expressed in eqn. 1 is essentially a longitudinal representation of modes, in the form $\varepsilon^{j\zeta z}$, travelling in the (perpendicular) x-direction. This representation then consists of a continuous spectrum with purely real eigenvalues varying between negative and positive infinity. The integral in eqn. 1 is usually solved by a deformation of the path of integration, in which case the simple representation in terms of a continuous real spectrum is usually destroyed.

Before attempting to perform a path deformation, the original path P along the real ζ-axis must be more rigorously defined with respect to the branch cut expressed by eqn. 2. It is then recognized that the semi-infinite character of the structure investigated here requires the specification of a radiation condition that is most conveniently stipulated as

$$\mathscr{I}(\kappa) = \kappa_i > 0 \quad . \quad . \quad . \quad . \quad . \quad (3a)$$

where $\mathscr{I}$ stands for 'the imaginary part of'. Eqn. $3a$ then implies that the waves are decaying properly in the cross-section as $x \to \infty$. Only the upper half of the κ-plane complies with this condition. The branch cut is then so chosen that this upper (proper) half of the κ-plane plots on to the top sheet of a two-sheeted Riemann ζ-plane; consequently, the lower (improper) half of the κ-plane plots on to the bottom sheet of the ζ-plane. The branch cuts are illustrated in Fig. 2(a), which shows the top sheet of the ζ-plane. It is noted that the cuts ($\kappa_i = 0$) are given from eqn. 2 in such a manner that the free-space medium considered here exhibits infinitesimal losses, i.e.

$$0 < \mathscr{I}k^2 \ll |k|^2 \quad . \quad . \quad . \quad . \quad . \quad . \quad (3b)$$

The integration in eqn. 1 is then properly carried out along the entire real ζ-axis in the top sheet of the 2-sheeted ζ-plane.

It is recognized that this way of choosing a branch cut is not unique; other possible methods have, in fact, been employed. However, the choice shown here has the advantage that the transverse representation obtained by a contour deformation, shown below, is a spectral one;[27] other choices for the branch cuts do not lead directly to this spectral representation. In addition, the present choice means that the entire top sheet in the ζ-plane complies with the radiation condition, unlike other choices wherein parts of both the top and bottom sheets agree with this radiation requirement.

2.2 The transverse spectral representation; propagation along the interface

A first approach to solving eqn. 1 is to transform it into a transverse representation of modes in the form $\varepsilon^{j\kappa x}$ propagating in the z-direction. This is effected by deforming the original path of integration P into the path P′ along a semicircle at infinity, as is shown in Fig. 2(a) for positive

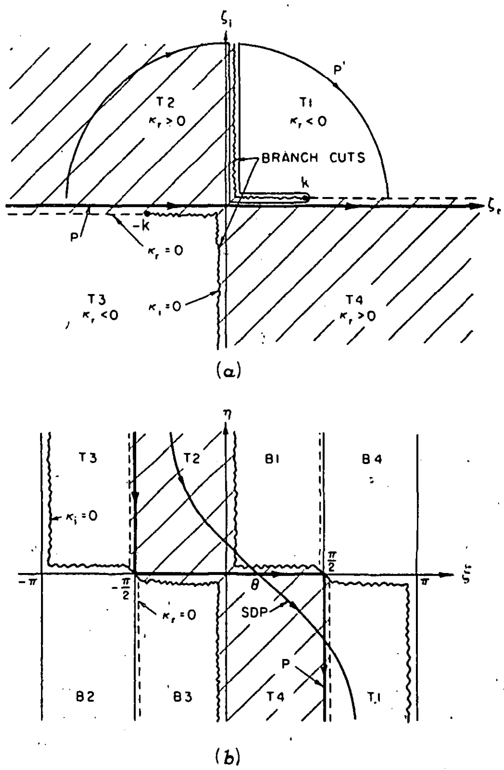

Fig. 2
Paths of integration and branch cuts
(a) Top sheet of ζ-plane
(b) Steepest-descent ϕ-plane

z; for negative z, the semicircle would be in the lower half of the top sheet of the ζ-plane. The semicircle at infinity contributes nothing to the integral; hence, by Cauchy's theorem for complex integration, the representation in eqn. 1 may be written as

$$G(x, z) = \frac{1}{2\pi}\left[\int_{-\infty}^{\infty}\left(f(\kappa)\varepsilon^{j\kappa x}\varepsilon^{j\zeta z}\frac{d\zeta}{d\kappa}\right)d\kappa + 2\pi j\,\Sigma\text{ Residues}\right] \quad . \; . \; . \; . \quad (4)$$

The integration in eqn. 4 is carried out along the entire real κ-axis and corresponds to a path around the branch cut in Fig. 2(*a*); also, residue contributions may be present because of possible pole singularities which occur in only the top sheet of the ζ-plane, i.e. the upper half of the κ-plane. These pole singularities are consequently classified as proper (or spectral) poles, since their fields correspond to waves which comply with the radiation condition of eqn. 3*a*. These waves are identified as the well-known 'surface waves'[1-5] or as the less familiar complex waves.[11-14] On the other hand, poles located in the bottom sheet of the ζ-plane, i.e. lower half of the κ-plane, are never captured by the deformed path P'; hence, they never contribute in this transverse spectral representation and are therefore classified as improper, or non-spectral.

It is realized that, while the longitudinal representation in eqn. 1 involves a continuous spectrum only, the transverse representation (eqn. 4) may, in addition, exhibit a discrete spectrum. The latter representation has therefore the advantage of exhibiting explicitly the discrete waves associated with a boundary interface. The continuous-wave spectrum is not bound at the interface and accounts for radiation; its field aspects were described by Brown[15] in terms of plane waves which either are propagated or decay along the interface.

Except that it explicitly shows a discrete spectrum, the integral in eqn. 4 is quite evidently of the same form as the one in eqn. 1 so that, at least for the continuous spectrum, little progress has been made in the actual solution of the field.

2.3 The steepest-descent representation

The steepest-descent representation is customarily employed to obtain an explicit solution for the field. Briefly, this involves a transformation

$$\zeta = k \sin\phi, \quad \kappa = k\cos\phi \quad . \; . \; . \; . \quad (5)$$

where $\phi = \xi + j\eta$ is the complex plane in which the steepest-descent integration is carried out. The transformations of eqn. 5 plot the entire 2-sheeted ζ-plane into a strip of the ϕ-plane, as shown in Fig. 2(b). It is noticed that each of the eight quadrants in the ζ-plane transforms into semi-infinite strips identified in the Figure by means of T (top) or B (bottom) and the quadrant number. The original path P is deformed into the steepest-descent path SDP which passes through the saddle point $\phi = \theta$ and is defined by

$$\cos(\xi - \theta)\cosh\eta = 1 \quad . \; . \; . \; . \quad (6)$$

It may then be shown that the integration of eqn. 1, computed along SDP, yields:

$$G_s(r, \theta) \sim k\,F(\theta)\,\frac{\varepsilon^{j(kr-\pi/4)}}{\sqrt{2\pi kr}} \qquad \text{for } \theta \neq \pm\frac{\pi}{2} \quad . \quad (7a)$$

$$G_s(z) \sim \frac{k}{2}\,F''\left(\pm\frac{\pi}{2}\right)\frac{\varepsilon^{j(k|z|-3\pi/4)}}{\sqrt{(2\pi|kz|^3)}} \qquad \text{for } \theta \simeq \pm\frac{\pi}{2} \quad .. \quad (7b)$$

where $\qquad F(\phi) = f(\kappa)\cos\phi$

In these equations, $F''\left(\pm\frac{\pi}{2}\right)$ denotes the second derivative of $F(\phi)$ with respect to ϕ, evaluated at $\phi = \pm\frac{\pi}{2}$; the $\sim$ sign indicates the fact that the eqns. 7 are asymptotic approximations which are valid when kr and $k|z|$ are considerably larger than unity. The significance of r and θ is shown in Fig. 1, these being, respectively, the radius vector and the polar angle of the field point in free space. It is noted that eqn. 7*b* refers to points at or very close to the interface. In contrast to the Cartesian form of the previous spectral representations, it is evident from eqns. 7 that the steepest-descent representation has a polar form with the observation point being represented by (r, θ) rather than (x, z). Also, the saddle point is given directly by the angle of observation θ.

The eqns. 7 are only a partial solution of the integral in eqn. 1, and they represent a contribution to the field which is referred to as the 'space wave'. Additional discrete contributions may be present because of poles of $F(\phi)$ which are located between the original path P and the deformed path SDP in the ϕ-plane. A typical pole contribution is obtained by applying the residue theorem to eqn. 1, which then yields for a pole at $\phi = \phi_p$

$$G_p(r, \theta) = \pm\, jk\frac{[F(\phi_p)]^2}{F'(\phi_p)}\,\varepsilon^{jkr\cos(\phi_p-\theta)}U(\theta, \theta_c) \quad . \; . \quad (8)$$

where the $\pm$ sign refers to the clockwise (+) or counter-clockwise (−) sense employed on the path essentially surrounding the pole used in the residue evaluation. The function $U(\theta, \theta_c)$ is a step function; it is unity if the pole lies between the paths P and SDP, and it vanishes if the pole is not thus captured. The angle θ_c denotes the 'definition angle' which distinguishes between regions of zero or non-zero contribution and is defined from eqn. 6 for $\phi = \phi_p$.

Since more than one pole may contribute to the field, the solution is given by

$$G(r, \theta) = G_s(r, \theta) + \sum_{p=1}^{N} G_p(r, \theta) \quad . \; . \; . \quad (9)$$

where N poles are assumed to be captured by the steepest-descent path. In contrast to the transverse spectral representation, poles which lie in the bottom sheet of the ζ-plane may now also contribute. These poles are sometimes captured by the steepest-descent path SDP which, over some of its extent, crosses into an improper part of the ζ-plane [the half-strips denoted by B in Fig. 2(*b*)] whenever $\theta \neq 0$. The steepest-descent representation is thus clearly not a spectral one.

In addition to the terms constituting $G(r, \theta)$ in eqn. 9, other terms may sometimes be required in order to obtain a more accurate result. These possible additional contributions may be due to the function $f(\kappa)$ necessitating the definition of additional branch cuts or correction terms [28, 29] for angles θ for which the steepest-descent path comes very close to the poles. Unless otherwise specified, it will be assumed in the following considerations that these additional terms may be disregarded, either because they are insignificantly small or because we exclude from the discussion all the specific angles θ for which these terms are not negligible. Under these restrictions, $G(r, \theta)$ in eqn. 9 then represents, via eqns. 7 and 8, a formal, complete and asymptotically approximate solution for the field at the interface and in the free-space region above it.

3 The nature of the fields contributed by poles

3.1 The transverse resonance relation

It was previously noted that pole contributions to the field can arise only from poles of $f(\kappa)$. It may also be recognized that the function $f(\kappa)\varepsilon^{j\kappa x}$ is the characteristic (resolvent) Green's function of the one-dimensional transverse problem in the x-direction. Consequently, all the poles of $f(\kappa)$ may be found conveniently by using the transverse resonance principle,[30] which, in the present case, means that these poles are given by the roots of

$$Z_i(\kappa) + Z_0(\kappa) = 0 \quad . \quad . \quad . \quad . \quad . \quad (10)$$

where $Z_i(\kappa)$ is the specified impedance function at the interface and $Z_0(\kappa)$ is the characteristic impedance of the semi-infinite transmission line which represents the free-space region.

The roots of eqn. 10 yield all the poles of $f(\kappa)$, and they correspond to all the eigenvalues of the spectral transverse representation if the radiation condition (eqn. 3a) is also satisfied. Those roots of eqn. 10 which do not satisfy this radiation condition are obviously improper eigenvalues, which, as poles of $f(\kappa)$, may account for non-spectral wave contributions. Both classes of root are treated in this Section; some general properties of the resulting waves are examined first, and the fields of the various types are then discussed separately.

3.2 General properties of pole contributions

The roots of eqn. 10, which appear as poles of $f(\kappa)$ in the κ-plane, have, in general, complex values. The location of a pole at $\phi = \phi_p$ will therefore be given by

$$\phi_p = \xi_p + j\eta_p \quad . \quad . \quad . \quad . \quad . \quad (11a)$$

$$\zeta_p = \zeta_{pr} + j\zeta_{pi} \quad . \quad . \quad . \quad . \quad . \quad (11b)$$

$$\kappa_p = \kappa_{pr} + j\kappa_{pi} \quad . \quad . \quad . \quad . \quad . \quad (11c)$$

where the subscripts r and i refer to the real and imaginary parts, respectively. Clearly, for every pole κ_p in the κ-plane there will be a pole pair ($+\zeta_p$ and $-\zeta_p$) in the ζ-plane and therefore a pole pair ($+\phi_p$ and $-\phi_p$) in the ϕ-plane, because of the $\pm$ signs in eqn. 2. This result follows from the assumed bi-directional characteristics of the structure and implies that two waves are excited and travel in the $+z$ and $-z$ directions, respectively; expressed differently, for problems of the type considered here, the two poles $+\zeta_p$ and $-\zeta_p$ correspond, respectively, to contributions in the positive- and negative-z regions of space in the transverse representation (eqn. 4). To distinguish between the poles in a pair, these are designated ζ_p', ζ_p'' or ϕ_p', ϕ_p'', where the primed quantities differ from the double-primed ones in sign only.

3.2.1 Characteristic angles

Owing to the symmetry of the geometry used, the fields are necessarily mirror-symmetric about the xy-plane. Consequently, only the positive region ($0 \leqslant \theta \leqslant \pi/2$) is dealt with, and all the following derivations refer to this region, unless it is expressly stated otherwise. The steepest-descent path SDP therefore varies between the path through the origin and that through $\theta = \pi/2$, denoted, respectively, by OSDP and LSDP$^+$, and shown in Fig. 3. In the Figure, the path LSDP$^-$ through $\theta = -\pi/2$ is also shown for reference, and it is noted that only poles in the region included between LSDP$^+$ and LSDP$^-$ may contribute. Since poles are seen to appear in pairs in the ϕ-plane, there will be a pair of angles of definition, θ_c', θ_c'', corresponding to each pole pair, ϕ_p', ϕ_p''; these pole pairs are seen to comply with $\phi_p' = -\phi_p''$, which leads to $\theta_c' = -\theta_c''$. To simplify future considerations, the angle of definition

$$\theta_c = \theta_c' = -\theta_c'' \quad . \quad . \quad . \quad . \quad . \quad (12)$$

will always be taken to refer to the pole $\phi_p = \phi_p'$ that corresponds to a wave which decays with increasing z, i.e. ϕ_p' complies with $\mathscr{I}\zeta_p' = \zeta_{pi}' > 0$, and is therefore located in one of the strips T1, T2, B1 or B2. The other pole ϕ_p'' in the pole pair is then located in one of the strips T3, T4, B3 or B4, respectively. For illustration, a pole pair, p', p'', is shown in Fig. 3, together with the critical steepest-descent path CSDP, which goes through the pole p' and determines the definition angle θ_c. With the convention of eqn. 12, it may be seen that for a contributing pole $\phi_p = \phi_p'$,

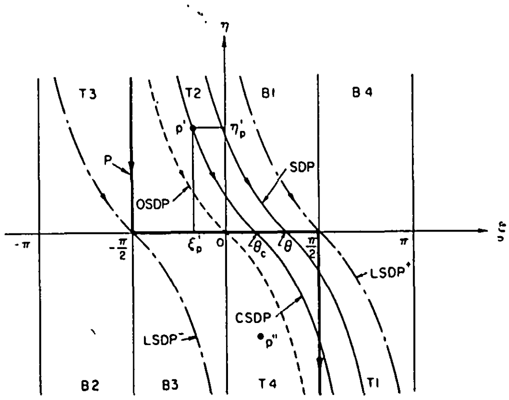

Fig. 3
Characteristic paths of integration in the steepest-descent ϕ-plane

$$\xi_p \leqslant \theta_c \leqslant \theta \leqslant \frac{\pi}{2} \quad \text{if } \eta_p > 0 \quad . \quad . \quad . \quad (13a)$$

$$\theta_c \leqslant \theta \leqslant \frac{\pi}{2} \leqslant \xi_p \quad \text{if } \eta_p < 0 \quad . \quad . \quad . \quad (13b)$$

where θ is understood to refer only to those angles for which the pole at ϕ_p contributes.

3.2.2 Field contours

For any angle θ within the range specified by eqns. 13, a pole contribution is obtained by taking the appropriate residue in eqn. 4, which yields a field

$$G_p(x, z) = G_0(\phi_p)\varepsilon^{j\kappa_p x}\varepsilon^{j\zeta_p z} \quad . \quad . \quad . \quad (14)$$

This result may be expressed in polar form either by using eqn. 8 or, alternatively, by applying eqns. 5 and 11 to eqn. 14, thus obtaining

$$G_p(r, \theta) = G_0(\phi_p)\varepsilon^{-\alpha_r r}\varepsilon^{j\beta_r r} \quad . \quad . \quad . \quad . \quad (15)$$

where

$$\alpha_r = k \sin(\theta - \xi_p) \sinh \eta_p \quad . \quad . \quad (16a)$$

$$\beta_r = k \cos(\theta - \xi_p) \cosh \eta_p \quad . \quad . \quad (16b)$$

and where $G_0(\phi_p)$ denotes the value of $G_p(x, z)$ or $G_p(r, \theta)$ at the origin. Since the angle θ is understood to refer to angles for which the pole at ϕ_p is captured by the path SDP, in agreement with eqns. 13, the step function $U(\theta, \theta_c)$ of eqn. 8 is omitted in eqns. 14 and 15.

The term α_r in eqn. 15 is a radial attenuation factor; if eqns. 13 are applied to eqn. 16a, it follows that $\alpha_r \geqslant 0$ for all angles in the region within which the pole contributes to the field. Consequently, the wave contributed by any complex pole is radially attenuated everywhere within its region of definition and is therefore a proper representation within this region. Note that this statement is true for both the proper and improper pole contributions.

If the phase and amplitude variations in eqns. 14–16 are now considered, the wave due to a single complex pole may be viewed, within its domain of definition, as a plane inhomogeneous wave which is propagated unattenuated and with a low phase velocity in a direction parallel to the radius vector at $\theta = \xi_p$. The amplitude of this wave is in exponential form, and from eqns. 16 it is clear that the equi-phase and equi-amplitude contours form orthogonal planes. It is noted that this orthogonality is independent of the particular boundary condition at the interface and holds whenever the free-space region is considered ideally lossless (a purely real value for k is implicit in eqns. 5 when they are used to obtain eqns. 16 from eqn. 15). It is also seen from eqns. 6 and 16 that, at the angle $\theta = \theta_c$, the wave travels with the speed of light but with a non-zero attenuation rate, i.e. $\alpha_r \neq 0$.

3.2.3 Local power flow

The real power flow $\boldsymbol{P}$ of a complex wave is found by evaluating the real part of the complex Poynting vector. The components of the vector $\boldsymbol{P}$ are then given as

$$P_x = C\kappa_{pr}|G_p(x, z)|^2 \quad . \quad . \quad . \quad . \quad (17a)$$

$$P_z = C\zeta_{pr}|G_p(x, z)|^2 \quad . \quad . \quad . \quad . \quad (17b)$$

where C is a positive real constant proportional to ϵ_0 (for E-modes) or μ_0 (for H-modes). When eqns. 17 are examined in conjunction with eqn. 14, it is clear that the power-flow lines are orthogonal to the equi-phase contours and are therefore parallel to the equi-amplitude contours. Also, the power-flow vector $\boldsymbol{P}$ always points in the direction of increasing phase in the free-space region.

3.2.4 Lossless structures

So far no restriction on losses has been specified for the boundary condition at the interface. If, however, this interface is such as to represent a lossless medium for $x \leqslant 0$, the input impedance $Z_i(\kappa)$ complies with the condition

$$Z_i^*(\kappa) = -Z_i(-\kappa^*) \quad . \quad . \quad . \quad . \quad (18)$$

where the asterisk represents the complex conjugate. The characteristic impedance $Z_0(\kappa)$ is given by

$$Z_0(\kappa) = \left.\begin{matrix} \kappa/\omega\epsilon_0 & \text{E-modes} \\ \omega\mu_0/\kappa & \text{H-modes} \end{matrix}\right\} \quad . \quad . \quad . \quad (19)$$

Introducing eqns. 18 and 19 into the transverse resonance condition (eqn. 10) we see that, if κ_p is a root of eqn. 10, $-\kappa_p^*$ is necessarily also a root. It therefore follows that poles in the integral representation of the field always appear in pairs (κ_p and $-\kappa_p^*$) in the κ-plane if the structures considered are lossless. Consequently, the poles then appear in groups of two pairs in the ξ- and ϕ-planes with symmetries which are indicated in Fig. 4 as follows:

Symmetry about the imaginary axis in the κ-plane.

Symmetry about both real and imaginary axes in the ζ-plane.

Symmetry about the origin in the ϕ-plane; in addition, because of the periodic nature of this plane, the poles are located symmetrically about any $\xi = (2n + 1)\pi/2$ axis and anti-symmetrically about any $\xi = n\pi$ axis.

The significance of the pole locations and their symmetries is made evident in the following Sections.

3.3 Proper complex modes in the transverse representation

Since the proper roots of the transverse resonance equation 10 are those which also satisfy the radiation condition of eqn. 3a, they represent discrete eigenvalues which form part of the complete spectrum of the transverse representation dealt with in Section 2.2. Although Section 3 deals mainly with the steepest-descent representation, it is appropriate for comparison to derive the shape of the fields as

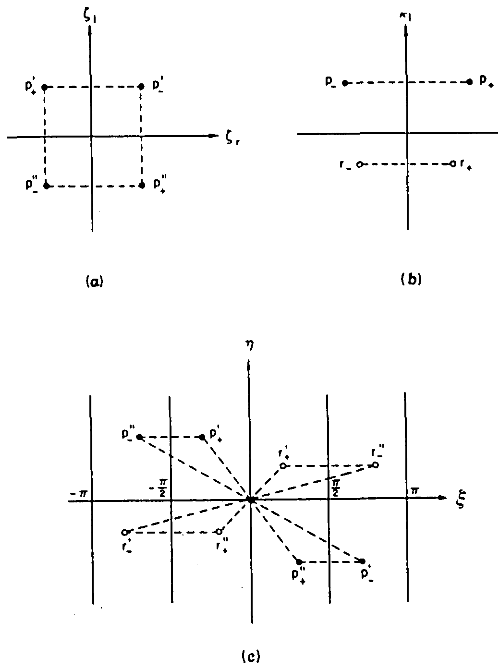

Fig. 4

Typical locations of poles for lossless configurations

(a) Top sheet of ζ-plane
(b) κ-plane
(c) ϕ-plane

Black dots and white circles denote, respectively, proper (spectral) and improper poles

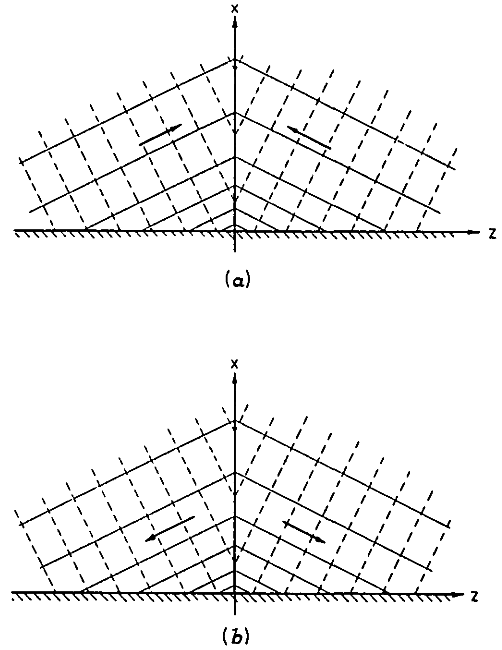

Fig. 5

Complex-wave fields in the transverse spectral representation

—— Equi-amplitude contours
- - - - Equi-phase contours
——→ Direction of power flow and increasing phase

(a) Field due to pole κ_{p+} in first quadrant of κ-plane
(b) Field due to pole κ_{p-} in second quadrant of κ-plane

modes in the transverse representation. These modes are evidently defined everywhere in space and are shown in Fig. 5, which is obtained by means of eqn. 14 while noting that ζ_p' and $\zeta_p'' = -\zeta_p'$ contribute in the positive and negative regions, respectively. Figs. 5(a) and 5(b) indicate the fields due, respectively, to a pole κ_{p+} in the first quadrant and a pole κ_{p-} in the second quadrant of the κ-plane; the amplitude behaviour is seen to be similar for the two cases but the power flow is different.

In lossless configurations, it was seen that the complex modes always appear in pairs with wave numbers κ_p and $-\kappa_p^*$, corresponding to $\pm\zeta_p$ and $\mp\zeta_p^*$. However, two modes ζ_i and ζ_j are not orthogonal[6, 31, 32] to each other if $\zeta_i = -\zeta_j^*$, and they must be considered together when their power is evaluated. As $|G_p(x, z)|^2$ in eqns. 17 has the same value for the contributions from both ζ_p and $-\zeta_p^*$, the power flow of these two waves taken together in eqns. 17 vanishes everywhere. Hence, no net real power is carried by complex modes in lossless configurations. This fact has already been recognized by others[12, 13] and is easily demonstrated[14] to be the only possibility consistent with conservation of energy. Thus, if the two separate fields shown in Figs. 5(*a*) and 5(*b*) are superimposed, it is seen that power flows in opposite directions in the two fields and therefore cancels out everywhere when the condition $\kappa_{p+} = -\kappa_{p-}^*$ is imposed. The resulting field is then in the form of an exponentially damped standing wave along any radius from the origin. Consequently, although no real power flow is present, stored energy is associated with proper complex modes in a manner similar to that for cut-off modes in conventional waveguides.

In lossy configurations, waves such as those shown in Fig. 5 may appear independently. Thus the Zenneck wave,[2, 3] which is supported by a plane lossy earth, has the same field as the one shown in Fig. 5(*b*). The power flow in such a wave is directed from the plane of the source into the interface and is understood to represent the power that is given up to compensate for the losses at and below the interface. The wave shown in Fig. 5(*a*) therefore represents a kind of backward Zenneck wave, since the power flow is into the plane of the source. The physical interpretation to be given of such a wave and power flow is questionable in the absence of any additional information; it is further complicated by the fact that in lossy configurations the total power flow is not given by the sum of the powers of each mode, since cross-coupling between the various modes occurs. However, power-flow interpretations are possible in a steepest-descent representation, and they are discussed in Section 4.

3.4 Proper (spectral) complex waves in the steepest-descent representation

In contrast to a modal representation like the one just considered, both the proper and improper poles may contribute in a steepest-descent representation. In order to distinguish between these two types of field, the former are referred to as spectral waves since they correspond to proper (spectral) modes in a transverse representation; the contributions due to improper poles are discussed in Section 3.5.

Although it contributes everywhere in space in a modal representation, a proper pole in a steepest-descent representation may define a field either in the entire space or in certain regions only, or it may even contribute nothing to the total field. These various possibilities are determined from the actual location of the pole in the complex ϕ-plane, and, in particular, from its relation to the curves LSDP and OSDP, as shown in Fig. 6. This Figure shows only the strip T2 in the ϕ-plane but is, nevertheless, illustrative of any strip. The curves in Fig. 6 are the path OSDP and the mirror image of the LSDP$^+$ path reflected about the η-axis; four regions are thus defined, whose properties are shown in the caption to Fig. 6, where v_{px} and v_{pz} are, respectively, the phase velocities of the wave in the x and z directions. The other features of the field contributed by a pole are determined by the strip in which this pole is actually located, as described below.

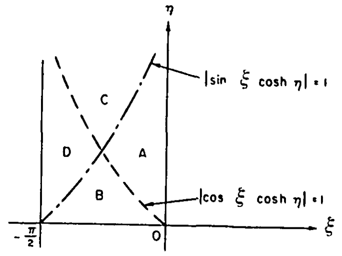

Fig. 6

Characteristic regions for complex poles, in the steepest-descent ϕ-plane

Phase velocities in the various regions

Region	v_{px}/c	v_{pz}/c
A	<1	>1
B	>1	>1
C	<1	<1
D	>1	<1

3.4.1 Configurations with losses

It was shown in Section 3.2 that two poles with origin symmetry are present in the ϕ-plane for every pole in the κ-plane. More than one such pole may exist in the κ-plane, but in lossy media their modes are, in general, orthogonal; unlike lossless configurations, no symmetrical pole pairs such as $\kappa_p, -\kappa_p^*$ are then necessary. Hence the fields of a single pole κ_p must be considered; these are shown in Figs. 7–10.

With the convention of Section 3.2.1, the location of a pole pair (p', p'') in the ϕ-plane is given by $\phi_p = \phi_p' = -\phi_p''$ and the angle of definition by $\theta_c = \theta_c' = -\theta_c''$, where the prime refers to the pole in the strips T1 or T2 and the double prime to the symmetrically located pole in the strips T3 or T4. The following four different field contributions are then possible:

(*a*) $0 < \sin\xi_p \cosh\eta_p < 1$. The pole is then situated to the right of the path LSDP$^+$ and it therefore never contributes in

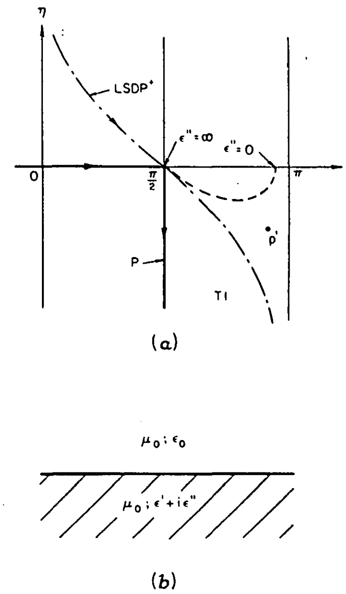

Fig. 7

Characteristics of a proper pole in lossy configurations with $0 < \sin\xi_p \cosh\eta_p < 1$

(*a*) Location in the ϕ-plane
---- Locus for Zenneck-wave pole
(*b*) Geometry for a lossy earth supporting a Zenneck wave

the steepest-descent representation, shown by the pole p' in Fig. 7(*a*). The characteristic region of such a pole corresponds to the areas A or B in Fig. 6, so that, in the transverse representation, there would be a wave whose velocity along the interface would be greater than the speed of light.

It is interesting to note that the pole yielding a Zenneck wave along a lossy earth [see Fig. 7(*b*)] is always of this type. The locus of such a pole is shown by the dashed line in Fig. 7(*a*) when the conductivity of the earth, represented by ϵ'', is varied between zero and infinity. Hence the Zenneck wave never appears as part of the total field in a steepest-descent representation, except as a correction term[33] when the pole is very near the steepest-descent path at $\theta = \pi/2$; this latter case occurs only when the conductivity of the earth is very large.

(*b*) $\sin \xi_p \cosh \eta_p > 1$. The pole is then located as indicated by p' in Fig. 8(*a*) and contributes a wave within an angle $0 \leqslant \theta_c \leqslant \theta \leqslant \pi/2$, shown in Fig. 8(*b*). The field contours of this wave are in agreement with the general characteristics discussed in Section 3.2.2, and, within its domain of definition, it looks like a Zenneck wave which travels along the interface with a phase velocity lower than the speed of light (the pole lies within an area corresponding to regions C and D in Fig. 6.) Waves of this type have been shown to exist along lossy dielectric slabs and other similar structures[1, 4, 34, 35]; they correspond to ordinary surface waves which are modified by the presence of loss in the guiding reactive surface.

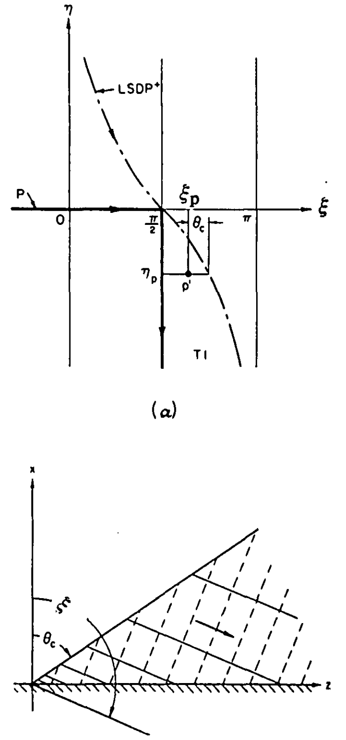

Fig. 8

Characteristics of a proper pole in lossy configurations with $\sin \xi_p \cosh \eta_p > 1$

(*a*) Location in the ϕ-plane
(*b*) Field contours

—— Equi-amplitude contours
– – – – Equi-phase contours
——> Direction of power flow and increasing phase

(*c*) $\cos \xi_p \cosh \eta_p > 1$. The position of the pole p' is shown in Fig. 9(*a*), and it is seen that it contributes a wave within an angle $0 \leqslant \theta_c \leqslant \theta \leqslant \pi/2$, as in (*b*) above. This pole is in the regions A or C of Fig. 6; consequently, the phase velocity of the wave in the x-direction is smaller than the speed of light. It is also seen that the pole p'' never contributes for angles in the positive-z region.

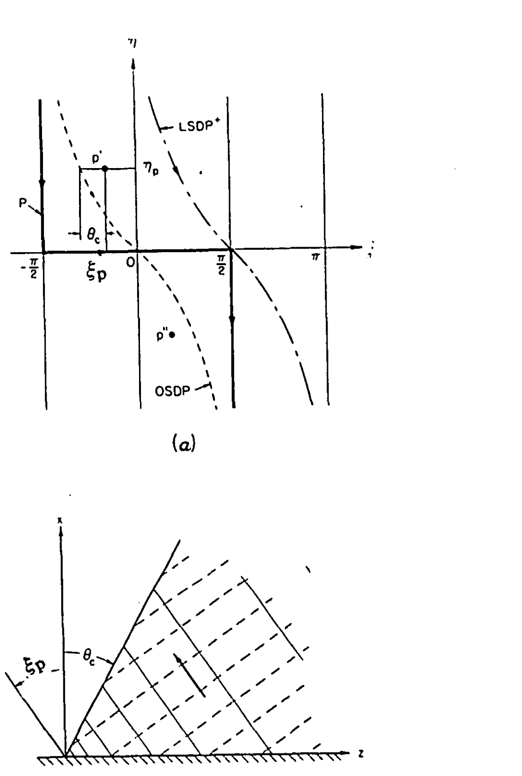

Fig. 9

Characteristics of a proper pole in lossy or lossless configurations with $\cos \xi_p \cosh \eta_p > 1$

(*a*) Location in the ϕ-plane
(*b*) Field contours

—— Equi-amplitude contours
– – – – Equi-phase contours
——> Direction of power flow and increasing phase

It is noted that, in contrast to the forward wave shown in Fig. 8(*b*), the wave shown in Fig. 9(*b*) travels into the plane of the source and is therefore a backward wave.

(*d*) $0 < \cos \xi_p \cosh \eta_p < 1$. Here the pole p' at ϕ_p contributes everywhere within an angle $-\pi/2 \leqslant \theta_c \leqslant \theta \leqslant \pi/2$, where $\theta_c < 0$, i.e. the domain of definition is greater than 90°. In the positive-z region the pole p'' at $\phi = -\phi_p$ also contributes within an angle $0 \leqslant \theta \leqslant -\theta_c$; this is in addition to the usual contribution from the pole p', indicated in Fig. 10. To find the total field in the positive-z region, it is noted that κ in eqn. 5, and hence $f(\kappa)$, are both independent of the sign of ϕ_p; if the positive or negative sign of the sense employed on the path essentially surrounding a pole involved in the residue evaluation of eqn. 4 is taken into account, it is obtained that

$$G_0(-\phi_p) = G_0(\phi_p) \quad . \quad . \quad . \quad . \quad (20)$$

The total field due to the pole pair ϕ_p, $-\phi_p$ becomes, from eqn. 14,

$$G_{pt}(x, z) = 2G_0(\zeta_p)\varepsilon^{j\kappa_p x} \cos \zeta_p z \quad \text{for } 0 \leqslant \theta \leqslant -\theta_c \quad . \quad (21)$$

As is shown in Fig. 9(*b*), the equi-phase and equi-amplitude field contours are no longer orthogonal within this region; these contours are now curved surfaces rather than planes, and they are parallel to each other for a translation in the

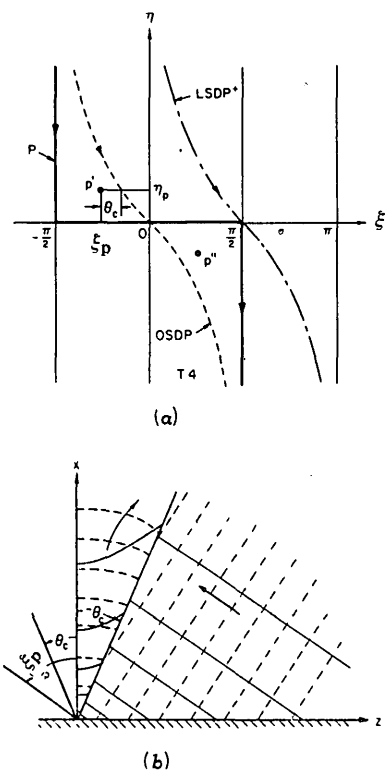

Fig. 10

Characteristics of a proper pole in lossy or lossless configurations with $0 < \cos \xi_p \cosh \eta_p < 1$

(*a*) Location in the ϕ-plane
(*b*) Field contours

—— Equi-amplitude contours
---- Equi-phase contours
⟶ Direction of power flow and increasing phase

x-direction. The pole is now located in one of the regions B or D of Fig. 6, so that the wave has a phase velocity in the x-direction greater than the speed of light.

Within the region $\theta_c < \theta < \pi/2$, the field has the form of a backward wave, as in (c). The field in the positive-z region due to the pole p'' constitutes an improper contribution since, in the transverse spectral representation, this pole takes account of proper fields in the negative-z region only. Nevertheless, this contribution is properly bounded in the steepest-descent representation, as was shown in the discussion immediately after eqns. 16. It should, of course, be recognized that if the source is unidirectional, rather than bi-directional, the pole p'' will not be present and the overlap shown in Fig. 10 will not occur; this aspect is taken up in Section 3.6.

3.4.2 Lossless configurations

An inspection of Fig. 4(c) indicates that, since poles appear in groups of four in lossless configurations, the path SDP may capture several of these poles simultaneously. The field contours will then be obtained by superposition of several of the diagrams discussed in the previous Section; the various fields are shown in Figs. 9–12.

Because poles now appear in all the strips T1 to T4, as shown in Fig. 4(c), it is convenient to take ϕ_p always to denote the pole located in the strip T2, since this pole is always included for some angles θ; thus, ξ_p, η_p and θ_c refer to a pole such as p'_+ in Fig. 4. Each of the regions A to D shown in Fig. 6 then determines a different type of field, as is described below. It is noted that, in the positive-z region of space, only the poles such as p'_+, p''_+ and p'_- in Fig. 4 may contribute, and that the pole p''_- yields no contributions to the field in that region.

(e) $\sec \xi_p < \cosh \eta_p < \operatorname{cosec}(-\xi_p)$. The pole p'_+ is in the region A of Fig. 6 and it alone contributes. This is a special case of the type (c) field discussed in Section 3.4.1 which occurs when the pole p'_- appears at the right of LSDP$^+$; the field contours are therefore similar to those shown in Fig. 9(b). The wave has the same properties as those discussed in Section 3.4.1(c), with a large phase velocity in the negative z-direction.

(f) $\cosh \eta_p < \sec \xi_p$ and $\cosh \eta_p < \operatorname{cosec}(-\xi_p)$. The pole p'_+ is in region B of Fig. 6, while the pole p'_- is to the right of LSDP$^+$ and therefore does not contribute; hence, this is a special case of the type (d) field discussed previously, in Section 3.4.1. The field contours are consequently similar to those shown in Fig. 10(b), and the wave has the same properties as those discussed in Section 3.4.1(d) with a large phase velocity in the negative z-direction.

(g) $\cosh \eta_p > \sec \xi_p$ and $\cosh \eta_p > \operatorname{cosec}(-\xi_p)$. The pole p'_+ is now in region C of Fig. 6 and the pole p'_- also contributes; however, the pole p''_+ does not. The region within which both p'_+ and p'_- contribute is given by $\theta_0 = \pi + 2\xi_p - \theta_c \leqslant \theta \leqslant \pi/2$, as shown in Fig. 11. Since

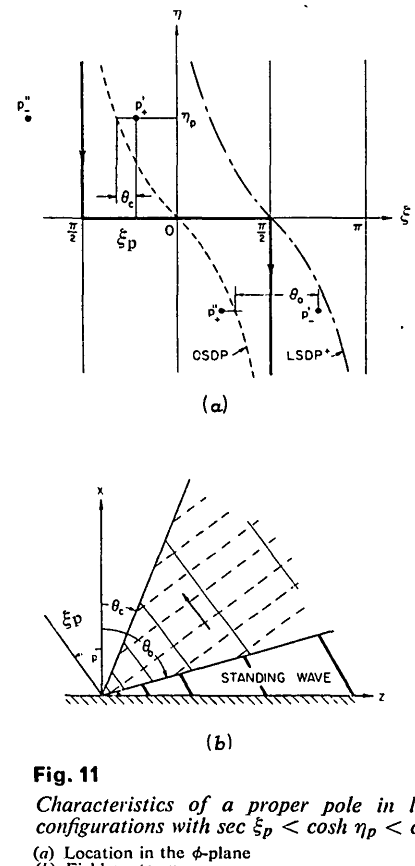

Fig. 11

Characteristics of a proper pole in lossless configurations with $\sec \xi_p < \cosh \eta_p < \operatorname{cosec}(-\xi_p)$

(*a*) Location in the ϕ-plane
(*b*) Field contours

—— Equi-amplitude contours
---- Equi-phase contours
⟶ Direction of power flow and increasing phase

contributions then occur from a pole pair (ζ_p, $-\zeta_p^*$), this case corresponds to that already considered in Section 3.3 where lossless structures are discussed, except that the region now exists only within $\theta_0 \leqslant \theta \leqslant \pi/2$; in this range, the field is therefore in the form of a standing wave which decays radially in an exponential fashion, as indicated in Fig. 11(b).

In the region in which only the pole p'_{+} contributes, the field is similar to that of (*e*) above, but the wave has low phase velocities in both the x and negative-z directions, rather than in the x-direction alone.

(*h*) $\operatorname{cosec}(-\xi_p) < \cosh \eta_p < \sec \xi_p$. The pole p'_{+} is in region D of Fig. 6, and it may easily be seen from Fig. 12(*a*)

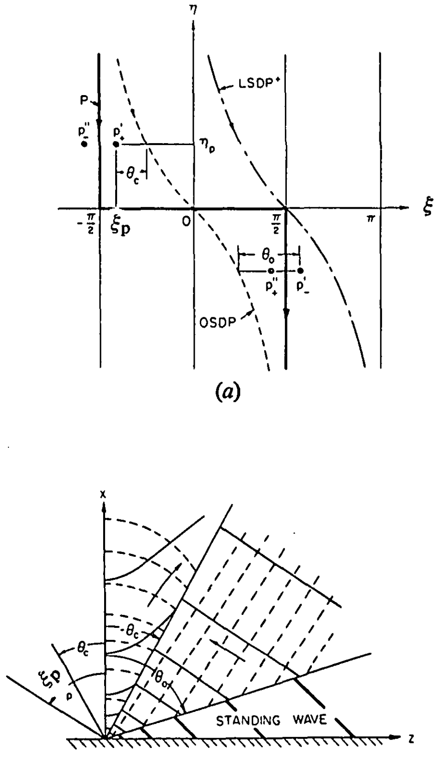

(*a*)

(*b*)

Fig. 12

Characteristics of a proper pole in lossless configurations with $\operatorname{cosec}(-\xi_p) < \cosh \eta_p < \sec \xi_p$

(*a*) Location in the ϕ-plane
(*b*) Field contours
—— Equi-amplitude contours
– – – Equi-phase contours
——→ Direction of power flow and increasing phase

that all the three poles p'_{+}, p'_{-} and p''_{+} contribute in various ranges of θ, with, however, not more than two poles contributing simultaneously. It is therefore clear that the resulting field contours are obtained as a combination of Figs. 10(*b*) and 11(*b*); this is shown in Fig. 12(*b*). Within the range $-\theta_c \leqslant \theta \leqslant \theta_0 = \pi + 2\xi_p - \theta_c$, where only the pole p'_{+} contributes, the field is in the form of a wave that is fast in the x-direction but slow in the negative z-direction.

It is noted that in all the lossless cases (Figs. 9–12) some local power flow is present, with energy being directed into a region defined by the radius vector at $\theta = \theta_c$, where, apparently, all this power is absorbed. Also, the proper complex waves for all the lossless cases are seen to be backward waves in all the regions in which only a single pole contributes. These power-transport features are examined further in Section 4.

3.4.3 Non-attenuated surface waves

The term 'surface wave' has sometimes been applied to a large class of related and non-related waves whose common denominator is a surface along which these waves propagate or to which they are bound. In the latter sense, all the spectral complex waves considered here are also surface waves, since they decay away from the interface; on the other hand, these complex waves were shown to propagate without decay along a radius vector at $\theta = \xi_p$ rather than along the interface ($\theta = \pm\pi/2$). However, for lossless structures, and if $\xi_p = \pm\pi/2$, the complex wave becomes a true surface wave in the sense that the propagation of its real power is along the interface only, with the wave decaying only transversely. Without wishing to stimulate discussion on the proper definition of a 'surface wave', we shall apply this term here only for the wave for which $\xi_p = \pm\pi/2$, and the name 'complex wave' will be retained for all the other cases ($\xi_p \neq \pm\pi/2$).

The condition $\xi_p = \pm\pi/2$, when taken in conjunction with eqns. 3*a* and 5, implies that ζ_p is purely real and κ_p positive imaginary, and that the wave is propagated unattenuated along the interface with a phase velocity less than the speed of light. To find the field contributed by a surface-wave pole, it is first noted that the path of integration P in eqn. 1 must be investigated in the neighbourhood of this pole, since both P and the pole itself lie on the real ζ-axis. The small-loss argument of eqn. 3*b* used for the branch cut in eqn. 2 is then applied to the incremental expression

$$\Delta\zeta = \frac{\partial\zeta}{\partial k}\Delta k$$

where $\Delta\zeta$ is the increment in ζ due to an increment Δk which corresponds to a loss-term addition to a lossless k. This relation may be written as

$$\Delta\zeta = \frac{\partial\zeta}{\partial\omega}\frac{\partial\omega}{\partial k}\Delta k = \frac{\omega}{\zeta}\frac{\partial\zeta}{\partial\omega}\frac{\zeta}{k}\Delta k$$

Noting that, for real ζ, ω/ζ is the phase velocity v_p, while $\partial\omega/\partial\zeta$ is the group velocity v_g of the surface wave, one sees that

$$\frac{\Delta\zeta}{\zeta} = \frac{v_p}{v_g}\frac{\Delta k}{k} \quad . \quad . \quad . \quad . \quad . \quad (22)$$

In agreement with eqn. 3*b*, the presence of small losses is now regarded as an incremental imaginary term on the otherwise unchanged real part of k^2. Since $\Delta k/k$ is then purely imaginary and positive, $\Delta\zeta/\zeta$ is likewise imaginary; however, the sign of $\Delta\zeta/\zeta$ depends on the nature of the wave, being positive for forward waves (v_p and v_g of the same sign) and negative for backward waves (v_p and v_g of opposite signs). Consequently, the path around surface-wave poles must be taken in the way shown in Figs. 13(*a*), (*c*) and (*e*), where f', f'' and b', b'' represent forward and backward surface-wave poles, respectively.

A comparison of Figs. 13(*d*) and (*f*) with Figs. 8 and 10 shows that the forward surface wave is a special case of the wave shown in Fig. 8, while the backward surface wave is a special case of the wave shown in Fig. 10, both these cases occurring when the losses become infinitesimal. True surface waves, therefore, are not limiting cases of a complex wave in a lossless medium with $\zeta_p \to \pm\pi/2$; if this were so, the two poles p''_{+} and p'_{-} in Fig. 12(*a*) would merge into a double pole so that $\theta_0 \to -\theta_c$, resulting in a standing-wave field everywhere and consequently no power transport. A surface wave, however, is due to a simple pole and generally carries a non-vanishing amount of power. Additional comments and clarifications of these aspects are given in Section 3.7.

When the power flow is examined for a backward surface wave, an apparently disturbing behaviour is noted: the power of a backward surface wave flows towards the plane of the source, in contrast to a forward surface wave for which power is flowing away from the source plane xy. However,

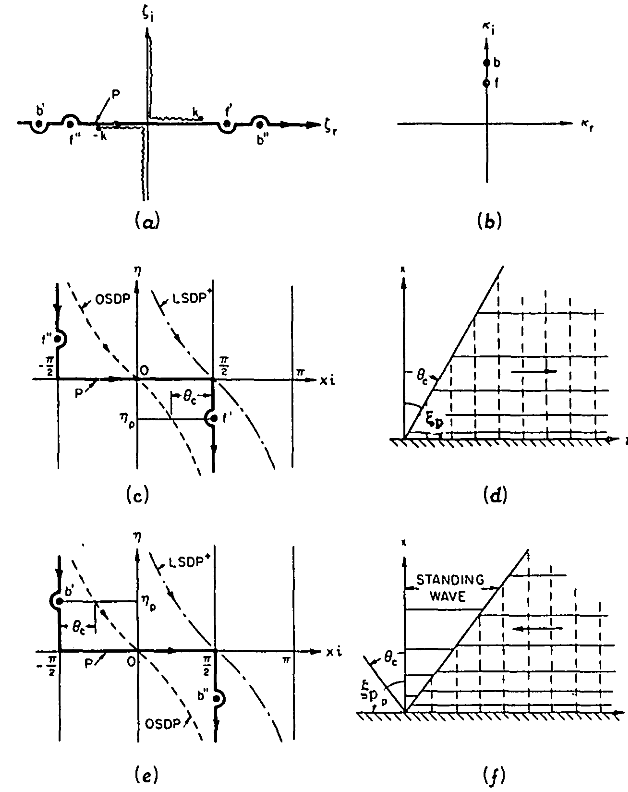

Fig. 13

Characteristics of true surface-wave poles

(*a*) Location and integration path in the ζ-plane
(*b*) Location in the κ-planes
(*c*) Location of a forward-wave pole in the ϕ-plane
(*d*) Field contours for a forward wave
(*e*) Location of a backward-wave pole in the ϕ-plane
(*f*) Field contours for a backward wave
—— Equi-amplitude contours
---- Equi-phase contours
—> Direction of power flow and increasing phase

when the transverse representation is used, the backward wave considered here is a proper mode by itself, which is independent of, and orthogonal to, all the other modes, in the same manner as a forward surface wave; consequently, the power flow directed into the plane of the source in Fig. 13(*f*) seems to be incompatible with passive configurations like those assumed here. This inconsistency may be resolved by realizing that the above direction of power flow represents only a local energy transfer. The phase and group velocities have opposite signs for a backward surface wave, so that if the phase increases in the negative *z*-direction as in Fig. 13(*f*), the group velocity, and hence the net energy transfer, points in the positive *z*-direction, i.e. away from the source. Consequently, a local energy transfer like the one shown in Fig. 13(*f*) indicates only that there must be an additional power flow in the opposite direction and with a magnitude such that the total net power is flowing out from the source plane. This additional power may flow at the interface itself or below it.

Although forward surface waves have already been extensively studied, it is only recently that backward modes have been found to exist in non-periodic structures[14, 18-25]; these studies showed that backward waves were possible in media which exhibited anisotropy[18-22] or transverse inhomogeneity,[18, 23, 24] in dispersive media,[14, 18, 25] or in combinations of these.[18] In Reference 14, which deals with a plasma layer in free space, it is shown that *E*-mode backward surface waves may exist, provided that the dielectric constant of the plasma is negative. The power flow in the free-space region is then, as shown in Fig. 13(*f*), but power flows in the opposite direction in the plasma layer, with a net power balance that is always flowing away from the source plane. It is, in fact, to be expected that backward waves that are modes by themselves would be possible only when a power-transfer mechanism similar to the above is present.

3.5. Improper complex waves

The improper solutions of the transverse resonance equation 10 have been investigated primarily for radiation from a special class of aerial.[10, 36-40] They are the origin of 'leaky waves' which are so called because of energy which leaks away continuously along the entire length of such aerials. However, it is shown in Section 4 that some of the proper complex waves also exhibit this power flow and should therefore also be classified as leaky waves. In order not to introduce confusion, the term 'leaky' will not be employed at this stage, and the waves dealt with in this Section will be denoted only as improper (non-spectral).

As has already been discussed in Section 2.2, a significant characteristic of non-spectral waves is that, being contributions from improper poles, they can never exist by themselves as modes in a spectral representation. They do, however, appear in certain spatial regions, but then as only part of the total field. Also, it is emphasized that their explicit presence is due to the particular representation, i.e. the steepest-descent method, which carries the integration into part of an improper Riemann sheet for some regions of space. It is, therefore, only this incursion into a non-spectral plane that is the origin of a contribution from an improper pole; in a transverse representation, such as the one given by eqn. 4, wherein each pole accounts for a spectral contribution everywhere in the space considered, the improper poles obviously cannot contribute, since their fields would not be regular at infinity. This means that the improper waves in the steepest-descent representation are actually part of the continuous spectrum and cannot be viewed as separate independently excited modes.

Improper poles are located in the quadrants B1 to B4, illustrated in Fig. 2(*b*). For a leaky-wave contribution to occur, however, the relevant pole must be captured by the steepest-descent path. It is then noted from Fig. 14(*a*) that only poles located in the strips corresponding to the quadrants B1 and B3 may contribute; moreover, from eqn. 6 applied to LSDP$^+$, only poles complying with

$$\sin \xi_p \cosh \eta_p < 1 \quad . \quad . \quad . \quad . \quad (23)$$

will be captured by the steepest-descent path and will yield improper wave contributions. From eqns. 13–16, the field of a leaky wave is shown to be that in Fig. 14(*b*), where it is noted that $0 < \xi_p < \theta_c \leqslant \theta \leqslant \pi/2$, so that the contribution always lies within an acute wedge, i.e. each leaky-wave pole of a pole pair ϕ_p', ϕ_p'' yields separate and non-overlapping contributions in the positive or negative regions of z or θ, respectively. Upon introduction of the appropriate values for the improper poles into eqn. 14, the fields are seen to decay with z but increase with x; the latter is due to the violation of the radiation condition of eqn. 3*a*. Nevertheless, the fields decay radially in all directions within the domain of definition of the leaky wave, as discussed in Section 3.2.2. With $\xi_p \leqslant \theta_c \leqslant \theta$ for an improper wave, it is found from eqns. 6 and 16*b* that $\beta_r = k$ at $\theta = \theta_c$ and $\beta_r < k$ for all other angles within the domain of definition. Hence, this wave is fast in all radial directions, including along the interface.

In contrast to proper (spectral) complex waves, the improper waves exhibit only one type of field, as shown in

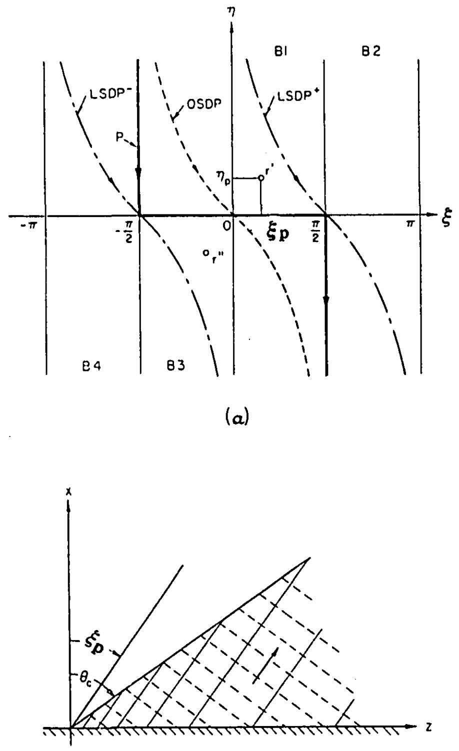

Fig. 14

Characteristics of an improper pole in lossy or lossless configurations

(*a*) Location in the ϕ-plane
(*b*) Field contours

—— Equi-amplitude contours
---- Equi-phase contours
——> Direction of power flow and increasing phase

Fig. 14(*b*), even when the configurations are lossless; this behaviour is due to the fact that, although four poles must be present simultaneously for lossless structures, only one pole contributes in the positive- and one in the negative-z regions. Also, the field of an improper wave is of the forward-wave type, in contrast to that of proper complex waves in lossless media which were seen to be mostly of the backward-wave type.

3.6 Unidirectional excitation

The roots of the transverse resonance equation 10 yield all the pole singularities of the characteristic Green's function independently of the source location and orientation. However, for certain special source configurations the waves due to some of these poles are excited with zero amplitude. In particular, a unidirectional excitation will effectively eliminate the wave due to one pole of a pole pair ϕ_p', ϕ_p''. Such a unidirectional excitation is obtained, for example, if a semi-infinite structure is end-fed by a closed waveguide, or if the source on an infinite structure consists of two line sources 90° out of phase with each other and spaced a quarter-wavelength apart.

For unidirectional excitations the symmetry about the xy-plane, which is implied in the discussions above and in Fig. 5 and Figs. 7–14, is destroyed. In examining the changes produced in the field distributions by eliminating one pole from a pole pair ϕ_p' ϕ_p'', let us assume that the pole p' at ϕ_p', which ordinarily contributes in the positive-z region, is the one that remains. An inspection of all the cases treated previously reveals that the field distributions shown in Figs. 5, 7, 8, 9, 11 and 13(*d*) are not affected by omitting the pole p'' at $\phi_p'' = -\phi_p'$, except that now the field contributed in the negative-z region vanishes instead of being symmetrical with the one shown in the Figures. It is noted that in all these cases no field overlap occurs in the region $|\theta| < |\theta_c|$, i.e. the pertinent pole contributes in the positive, or negative, region of z only.

Now consider the case shown in Fig. 10 when it is assumed that the pole p'' is absent. The situation will then be that shown in Fig. 15, which illustrates the fact that the pole contribution extends in a wedge larger than 90°. The fields of Figs. 12 and 13(*f*) are modified similarly, and, since they differ only in minor details from those shown in Fig. 15, they are not separately illustrated.

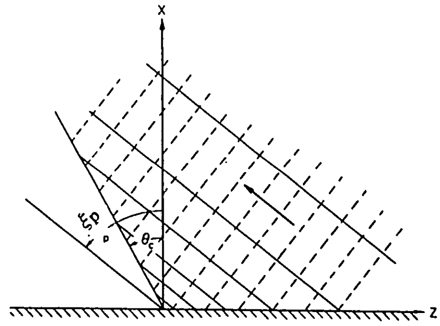

Fig. 15

Field due to unidirectional excitation of the structure for which a bi-directional excitation produces the field of Fig. 10(b)

An important practical case that corresponds to Fig. 15 is that of backward radiation from an array or a periodically modulated slow-wave structure. The radiation is then due to a space harmonic of the mode rather than the total mode itself; the wave is thus an example of a 'quasi-mode' defined by Karbowiak.[16] The interesting aspect is that this backward radiation is spectral and is not due to an improper wave, as is the forward radiation from the same space harmonic on the same structure; the change from backward to forward radiation is obtained by simply increasing the operating frequency. Further details of this backward radiation and its relation to periodic structures are presented elsewhere.[41]

3.7 Pole loci in the complex planes

All the poles considered here represent roots of the transverse resonance relation (eqn. 10), which is properly regarded as an equation to be solved for the variable κ. It is realized, however, that eqn. 10 also contains other variables characterizing the specific geometry involved or the physical characteristics of the media at $z \leqslant 0$, which specify $Z_i(\kappa)$. These additional variables appear as parameters in eqn. 10, and if they vary, the roots of the transverse resonance relation must also vary; also, because the functions involved are analytical, a particular root is expected to vary continuously and to appear as a continuous locus when plotted in the complex κ-plane while one of the parameters is varied continuously. Such a locus has already been shown in Fig. 7(*a*) in connection with the Zenneck wave.

A more interesting illustration[14, 42] is given in Fig. 16(*b*), which shows part of the κ-plane pole locus corresponding to the homogeneous and isotropic plasma slab shown in Fig. 16(*a*). The plasma medium is characterized by a relative dielectric constant $\epsilon_p = 1 - (\omega_p/\omega)^2$; when the frequency varies between zero and infinity, and all other parameters are kept constant, the solutions to the transverse resonance

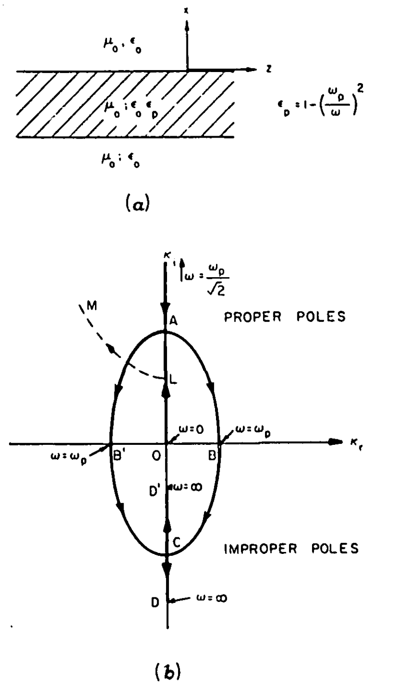

Fig. 16
Pole locations for a plasma slab
(*a*) Geometry and characteristics of the slab
(*b*) Locus of poles in the κ-plane as a function of ω, with fixed geometry

relation move in the direction shown by the arrows on the locus in Fig. 16(*b*). At low frequencies, two orthogonal true surface-wave poles move along the imaginary axis; at a critical frequency, they merge at the point A and then evolve into a pair of degenerate complex poles which produce two proper complex waves. The latter poles move symmetrically along AB and AB′, respectively; following the path AB, the pole reaches the real axis at B and then proceeds along BC, which is in a region on the improper (bottom) Riemann sheet of the ζ-plane. Consequently, the loci BC and B′C represent improper complex-wave poles; these reach the imaginary axis at C, where a double pole is again present. As the frequency is increased further, the poles separate and move along the imaginary axis, taking the form of improper surface-wave poles which never contribute in the steepest-descent representation; they appear as improper poles on the $\xi = \pi/2$ axis for $\eta > 0$ in the steepest-descent plane, and are therefore never captured.

The above example is useful in that it shows that, as a particular parameter in a given problem is varied, the nature of a complex pole may change continuously and can take the form of each of the types of pole discussed above.

To fill in the picture further, the dashed line LM in Fig. 16(*b*) shows part of the locus of a pole when the frequency is fixed and losses are progressively introduced in the plasma region; the surface-wave pole at L in the lossless case then changes into a complex pole along LM for the lossy case, in which the complex pole is no longer part of a symmetrical pair. This also illustrates the behaviour of a true surface-wave pole as the limiting case at L of a complex pole on LM when losses vanish; this is contrasted to the case at A which represents a double pole owing to the merging of a complex pole pair along AB and AB′, respectively. We recall that AB′ still represents a standing-wave field with no power transport. It is also noted that, as the frequency is reduced, the double pole at A separates into two poles on the imaginary axis which, in the transverse spectral representation, yield two orthogonal true surface waves, provided that no losses are present. However, if losses occur, these two poles appear as complex poles with a total power flow which can no longer be evaluated by taking the contribution of each pole separately.[6]

4 Power flow of complex waves

In the previous Sections, the physical aspects of the power flow of complex waves were dealt with summarily, and only non-attenuating surface waves were described in detail. These surface waves were seen to present the already familiar picture of a power transport strictly along the interface, with energy being carried away from the source.

When complex waves were considered in a transverse representation, their power transport in lossless structures was shown to be zero. In lossy configurations, power considerations are difficult, since mode orthogonality does not preclude power coupling between different discrete modes and between these and the continuous spectrum. One is therefore left only with the possibility of considering the entire field, and this approach is complicated by the fact that, in a longitudinal or transverse spectral representation, the contribution from the continuous spectrum is not usually known explicitly.

The above difficulty does not appear in the steepest-descent representation, in which the total field is known to be given by a cylindrical wave, pole contributions and possibly other partial fields, as discussed in conjunction with eqn. 9. It is then possible to present an adequate picture of the mechanism of power transport of both the complex waves and the space wave. This approach also has the advantage that the far field is shown to be strongly influenced by the presence or absence of complex waves.

To facilitate the discussion, lossless configurations are treated first. Also, the total field is considered to consist only of the space wave and pole contributions; any other terms are temporarily disregarded. If true surface waves are present, they will account for energy being carried along the interface away from the source, as is seen in Fig. 13. The power flow of complex waves is shown in Figs. 9–12 and 14, which describe all the possible contributions to the total field from complex poles in a lossless structure; it is then seen that in all these cases energy is directed into a region bounded on one side by $\theta = \theta_c$, where the power seems to be completely absorbed. Of course, this phenomenon must be interpreted in conjunction with the entire steepest-descent representation; the fields shown in Figs. 9–14 are only partial fields, and all energy considerations must relate to the total field. Energy is thus given up from the complex wave to the space wave everywhere along the radius at $\theta = \theta_c$. In a similar fashion, in the cases shown in Figs. 10 and 12, energy is given up from the space wave to the complex wave at $\theta = \theta_0$; θ_0 is, however, only an intermediate stage, since ultimately all the energy of the complex wave is given up to the space wave. Finally, it is realized that the space wave itself carries all its power into the radiation field so that the entire real power of the complex wave in the steepest-descent representation is converted into radiation.

To the above qualitative and pictorial discussion, a quantitative consideration should be added. The importance of a complex wave is greatest when it is strongly excited; under that condition the energy generated by the source is initially given up mainly to the complex wave, while the space wave is relatively weak in the neighbourhood of the source. Nevertheless, at large distances from the source, only the space wave is effectively present since it decreases as $r^{-1/2}$, compared with the complex wave which decays exponentially in all radial directions. To be consistent with conservation of energy, the power initially in the complex wave must appear ultimately in the space wave at large distances. However, the energy of the complex wave travels in a direction parallel to a radius vector at $\theta = \xi_p$, while the energy of the space wave travels everywhere radially, to a first approximation. The energy transfer must therefore occur in a region given closely by $\theta = \theta_c$, from which the power given up by the complex wave then proceeds radially outwards into the radiation field. Since it was initially assumed that the main part of the energy was in the complex wave, it follows that a radiation peak is expected in this case at an angle given approximately by θ_c.

To summarize the above results: when a complex wave is strongly excited, its power is carried into the radiation field via the space wave and results in a radiation peak at an angle close to the definition angle of that complex wave. Clearly, if more than one complex wave is strongly excited, several such radiation peaks may be expected. Also, if a complex wave is only weakly excited, its importance in the total field is insignificant and it is to be expected that a weak radiation peak will then appear, if a peak appears at all.

It is noted that the above discussion did not distinguish between proper (Figs. 9–13) and improper (Fig. 14) waves. Radiation at an angle close to θ_c has previously been associated with improper leaky waves along leaky-wave aerials, but this behaviour is seen here to hold for both types of complex wave. The term 'leaky' should therefore, strictly speaking, be extended to include all the complex waves which exhibit this power-flow feature. The fact that some waves are proper and some are not is seen to be a formal distinction; actually, all the complex wave types are leaky in lossless structures, and it is only when losses are present that another, non-radiating, type of complex wave is possible. The latter type is shown in Fig. 8, while the waves of Figs. 9–12 are in the leaky category.

To complete the picture, lossy configurations are discussed next. For this purpose, let us examine a structure for which a complex pole pair κ_p, $-\kappa_p^*$ occurs when no losses are present; the field is then in one of the forms shown in Figs. 9–12, which were seen to account for energy transfer into the radiation field. If small losses are now introduced, the two poles move slightly in the κ-plane but are no longer symmetrically located, and so their fields cannot be simply superimposed. Then one has to deal with two separate partial fields which can be in the form of the fields shown in Figs. 8, 9, 10 and 14 and discussed in Sections 3.4.1 and 3.5. The fields in Figs. 9, 10 and 14 have already been discussed and their energy transfer has been seen to be into the radiation field only. The only other type of field is the one in Fig. 8, which can only occur in lossy configurations; then, however, the direction of power is into the interface and clearly compensates for the assumed losses. If these losses are now increased further, instead of remaining infinitesimal, the two poles continue to move in the complex κ-plane. Nevertheless, the qualitative aspects of the fields in Figs. 8, 9, 10 and 14 do not vary with these changes in the locations of the poles, and so power still goes into radiation and into the losses of the given structure.

All the above arguments are unaffected if unidirectional excitations are considered, as may be verified by an inspection of Fig. 15.

A final remark is appropriate about partial fields other than those due to the saddle point (space wave) or pole contributions. It was noted in the discussion of eqn. 9 that other possible terms may be present which yield types of field other than those given by eqns. 7 and 8; in problems involving an interface of the type considered here, these additional contributions appear as correction terms to eqn. 9 which are important in specific restricted regions only, such as those given by the neighbourhood of the angles θ_c or θ_0. The purpose of these terms is to provide a progressive and continuous transition between two regions dominated by fields of different spatial variation. Thus, to give an example, a field strongly dominated by a complex wave, which has an exponential radial variation, must transform to a cylindrical $r^{-1/2}$ variation across θ_c; this transition is smoothly effected by means of the fields due to the correction terms. Apart from making their presence felt in restricted regions, these additional fields have no effect on the features considered above and indicate only that power is exchanged smoothly between the space wave and complex waves, and that this occurs within a finite small sector near θ_c, rather than abruptly at θ_c.

5 Conclusion

The waves that may form part of the field above a guiding structure have been examined and their features and physical aspects have been described in detail. It has been shown that all the waves due to poles in the integral representation of the field have in common an exponential field-dependence, and that these partial fields may be regarded as slow plane inhomogeneous waves which, in general, travel at an angle to an interface. The steepest-descent representation was used extensively in the discussion since it enables one to express the field in asymptotic form for angular regions of space within which either the space-wave or the pole-wave contributions may be dominant.

If the structure supporting the field is lossless, the following types of pole contribution may be present above an interface:

(*a*) True surface waves which travel without attenuation along the interface and decay normally away from it; they are characterized by a real propagation wave number, and they may carry a net amount of real power. These waves may be either forward or backward, with phase and group velocities in the same or the opposite direction, respectively.

In addition, waves with complex wave numbers may also be present; however, in lossless media, it was shown that such waves must occur in pairs, with one possessing a forward and the other a backward character. It is possible to distinguish between two types of these waves:

(*b*) Proper (spectral) complex waves, in lossless configurations, which decay both along and normal to the interface. These waves are proper modes and, as such, they are part of the discrete spectrum associated with the particular interface; the forward and backward waves in a wave pair are actually two degenerate modes which couple in such a manner that cancellation of real power occurs in a spectral representation. In a steepest-descent representation, however, local power transport exists and is mainly backward.

(*c*) Improper complex waves, in lossless configurations, which decay along the interface but increase in a direction perpendicular to it. These waves are not proper modes and may be defined in restricted regions only. They are therefore not part of the spectrum and occur only in non-spectral representations, such as the steepest-descent; then, only one of the waves in a pair contributes, this being always the forward one.

When the configurations considered are lossy, the waves can have complex wave numbers only, and they do not necessarily occur in pairs. The following types are then possible:

(*d*) Proper complex waves, in lossy configurations, which decay away from the source in the same manner as the waves under (*b*) above and are also spectral contributions. However, both as modes in the transverse representation or as waves in the steepest-descent representation, they may account for two kinds of power transfer: the forward type carries energy to compensate for losses while the backward type loses its energy to the radiation field. These waves may be subdivided into:

(i) Complex waves which, as losses are reduced to zero, become true surface waves of type (*a*);
(ii) Complex waves which, as losses vanish, become complex waves of type (*b*).

(*e*) Improper complex waves, in lossy configurations, whose field behaviour and other properties are indistinguishable from those of type (*c*).

Of the five types (*a*)–(*e*) enumerated above, the following have been known for some time:

The forward surface waves of type (*a*) were shown to travel along dielectric slabs and similar stratified media.

The leaky waves of type (*c*) or (*e*) were shown to appear in certain field representations and their importance in radiation phenomena was demonstrated.

The proper complex waves of type (*d*)(i) form the earliest known type of wave due to poles in the integral representation; in the later literature, they are termed 'surface waves' and have been shown to exist at the interface of media if some losses are present.

The other types of wave were found only recently and their presence was associated with anisotropic or dispersive media and also with some types of inhomogeneity in the cross-section of the guiding system; they may be classified as follows:

The backward surface wave of type (*a*) was shown to be present, as an independent mode, in ferrite and plasma guides, as well as in a circular guide containing a concentric dielectric rod which supports hybrid modes.

The proper complex waves of type (*b*) and, by extension, those of type (*d*)(ii) were shown to exist in structures containing ferrites or plasma.

The classification of all these waves into the five types (*a*) to (*e*) places their various features in proper perspective and emphasizes their interrelations. In particular, it is emphasized that the waves of types (*b*), (*c*), (*e*) and the backward variety of the wave of type (*d*) account for an energy transfer into the radiation field and, in this respect, are actually leaky waves, a term previously restricted to the waves of types (*c*) and (*e*) only. It is therefore suggested that this category should be extended to include all these waves and thus distinguish them from the forward variety of the wave of type (*d*), which alone represents the category of waves that carry energy to compensate for losses in the system.

The energy leakage into the radiation field was shown qualitatively to occur at a specific angle and in such a manner that it may produce radiation peaks. This aspect is dealt with quantitatively and in greater detail in a companion paper.[26]

6 Acknowledgment

The study reported herein was sponsored by the United States Air Force Cambridge Research Laboratories, under Contract No. AF19(604)–7499.

7 References

1 SOMMERFELD, A.: 'Über die Fortpflanzung elektrodynamischer Wellen längs eines Drahtes', *Wiedermann Ann. Phys. Chem.*, 1899, **67**, p. 233

2 ZENNECK, J.: 'Über die Fortpflanzung ebener elektromagnetischer Wellen längs einer ebenen Leiterflache', *Ann. Phys. (Leipzig)*, 1907, **23**, p. 846

3 BARLOW, H. M., and CULLEN, A. L.: 'Surface waves', *Proceedings I.E.E.*, 1953, **100**, Part III, p. 329

4 GOUBAU, G.: 'Waves on interfaces', *Trans Inst. Radio Engrs*, 1959, **AP–7**, Special Supplement, p. S140

5 BARLOW, H. E. M.: 'Surface waves: a proposed definition', *Proceedings. I.E.E.*, 1960, **107 B**, p. 240

6 ADLER, R. B.: 'Properties of guided waves on inhomogeneous cylindrical structures', *Proc. Inst. Radio Engrs*, 1952, **40**, p. 339

7 BARLOW, H. E. M., and KARBOWIAK, A. E.: 'An experimental investigation of axial cylindrical surface waves supported by capacitive surfaces', *Proceedings I.E.E.*, 1955, **102 B**, p. 313

8 ZUCKER, F. J.: 'The guiding and radiation of surface waves', Symposium on modern advances in microwave techniques, Polytechnic Institute of Brooklyn, New York, 1954, p. 403

9 MARCUVITZ, N.: 'On field representations in terms of leaky modes or eigenmodes', *Trans Inst. Radio Engrs*, 1956, **AP–4**, p. 192

10 GOLDSTONE, L. O., and OLINER, A. A.: 'Leaky wave antennas: Part I—rectangular waveguides', *ibid.*, 1959, **AP–7**, p. 307

11 Discussion on Button, K. J., and Lax, P.: 'Theory of ferrites in rectangular waveguide', *ibid.*, 1956, **AP–4**, p. 573

12 TAI, C. T.: 'Evanescent modes in a partially filled gyromagnetic rectangular waveguide', *J. appl. Phys.*, 1960, **31**, p. 220

13 CHORNEY, P.: 'Power and energy relations in bidirectional waveguides', Symposium on electromagnetic and fluid dynamics of gaseous plasma, Polytechnic Press, New York, 1961, p. 195

14 TAMIR, T., and OLINER, A. A.: 'The spectrum of electromagnetic waves guided by a plasma layer', *Proc. Inst. Radio Engrs* (to be published)

15 BROWN, J.: 'The types of wave which may exist near a guiding surface', *Proceedings I.E.E.*, 1953, **100**, Part III, p. 363

16 KARBOWIAK, A. E.: 'Some comments on the classification of waveguide modes', *ibid.*, 1959, **107 B**, p. 85

17 KARBOWIAK, A. E.: 'Radiation and guided waves', *Trans Inst. Radio Engrs*, 1959, **AP–7**, Special Supplement, p. S191

18 TRIVELPIECE, A. W.: 'Slow wave propagation in plasma waveguides', California Institute of Technology, Electron Tube and Microwave Laboratory, Technical Report No. 7, 1958

19 TRIVELPIECE, A. W., and GOULD, R. W.: 'Space charge waves in cylindrical plasma columns', *J. appl. Phys.*, 1959, **30**, p. 1784

20 BRESLER, A. D.: 'The far fields excited by a point source in a passive dissipationless anisotropic uniform waveguide', *Trans Inst. Radio Engrs*, 1959, **MTT–7**, p. 282

21 SEIDEL, H., and FLETCHER, R. C.: 'Gyromagnetic modes in waveguides partially loaded with ferrite', *Bell Syst. tech. J.*, 1959, **38**, p. 1427

22 TRIVELPIECE, A. W., IGNATIUS, A., and HOLSCHER, P.C.: 'Backward waves in longitudinally magnetized ferrite rods', *J. appl. Phys.*, 1961, **32**, p. 259

23 CLARRICOATS, P. J. B., and WALDRON, R. A.: 'Non-periodic slow-wave and backward-wave structures', *J. Electronics and Control*, 1960, **8**, p. 455

24 CLARRICOATS, P. J. B.: 'Backward waves in waveguides containing dielectric', *Proceedings I.E.E.*, 1961, **108 C**, p. 496

25 OLINER, A. A., and TAMIR, T.: 'Backward waves on isotropic plasma slabs', *J. appl. Phys.*, 1962, **33**, p. 231

26 TAMIR, T., and OLINER, A. A.: 'Guided complex waves: Part II—Relation to radiation patterns' (see next page)

27 COLLIN, R. E.: 'Field theory of guided waves' (McGraw-Hill, 1960). Section 11.8

28 VAN DER WAERDEN, B. L.: 'On the method of saddle points', *Appl. sci. Res.*, 1951, **B2**, p. 33

29 OBERHETTINGER, F.: 'A modification of Watson's lemma', *J. Res. Nat. Bur. Stand.*, 1959, **63B**, p. 15

30 MARCUVITZ, N.: 'Field representations in spherically stratified regions', *Communic. Pure appl. Math.*, 1951, **4**, p. 263

31 WALKER, L. R.: 'Orthogonality relations for gyrotropic wave guides', *J. appl. Phys.*, 1957, **28**, p. 377

32 BRESLER, A. D., JOSHI, G. H., and MARCUVITZ, N.: 'Orthogonality properties for modes in passive and active uniform wave guides', *ibid.*, 1958, **29**, p. 794

33 FELSEN, L. B., and MARCUVITZ, N.: 'Modal analysis and synthesis of electromagnetic fields', Polytechnic Institute of Brooklyn, Microwave Research Institute, Report No. PIBMRI–841–60, 1961

34 ATTWOOD, S. C.: 'Surface wave propagation over a coated plane conductor', *J. appl. Phys.*, 1951, **22**, p. 504

35 WAIT, J. R.: 'Excitation of surface waves on conducting, stratified and dielectric clad surfaces', *J. Res. Nat. Bur. Stand.*, 1957, **59**, p. 365

36 RUMSEY, V. H.: 'Theory of traveling wave slot antennas', *J. appl Phys.*, 1953, **24**, p. 1358

37 HONEY, R. C.: 'A flush-mounted leaky wave antenna', *Trans Inst. Radio Engrs*, 1959, **AP–7**, p. 320

38 ZUCKER, F. J.: 'Surface- and leaky-wave antennas', in Jasik, Henry (Ed.): 'Antenna engineering handbook' (McGraw-Hill, 1961). Ch. 16

39 HARRINGTON, R. F.: 'Propagation along a slotted cylinder', *J. appl. Phys.*, 1953, **24**, p. 1336

40 GOLDSTONE, L. O., and OLINER, A. A.: 'Leaky wave antennas: Part II—Circular waveguides', *Trans Inst. Radio Engrs.*, 1961, **AP–9**, p. 280

41 HESSEL, A., and OLINER, A. A.: 'Radiation from planar periodic structures', submitted for publication in *Trans Inst. Radio Engrs*

42 TAMIR, T., and OLINER, A. A.: 'The influence of complex waves on the radiation field of a slot-excited plasma layer', *Trans Inst. Radio Engrs*, 1962, **AP–10**, p. 55